UNICA UNIVERSITÀ DEGLI STUDI DI CAGLIARI

Resveratrol and artemisinin eudragit-coated liposomes: a strategy to tackle intestinal tumors

Carla Caddeo [a,§,*], Morena Gabriele [b,§], Amparo Nácher [c,d], Xavier Fernàndez-Busquets [e,f], Donatella Valenti [a], Anna Maria Fadda [a], Laura Pucci [b,*], Maria Manconi [a]

[a] Dept. of Scienze della Vita e dell'Ambiente, Sezione di Scienze del Farmaco, University of Cagliari, Via Ospedale 72, 09124 Cagliari, Italy

[b] Institute of Agricultural Biology and Biotechnology, CNR Pisa, Via Moruzzi 1, 56124 Pisa, Italy

[c] Dept. of Pharmacy and Pharmaceutical Technology, Faculty of Pharmacy, University of Valencia, Vicente Andrés Estellés s/n, 46100 Valencia, Spain

[d] Instituto Interuniversitario de Investigación de Reconocimiento Molecular y Desarrollo Tecnológico (IDM), Universitat Politècnica de València, Universitat de València, Valencia, Spain

[e] Nanomalaria Group, Institute for Bioengineering of Catalonia (IBEC), The Barcelona Institute of Science and Technology, Baldiri Reixac 10-12, Barcelona E08028, Spain

[f] Barcelona Institute for Global Health (ISGlobal), Hospital Clínic-Universitat de Barcelona, Rosselló 149-153, Barcelona E08036, Spain

[§] These authors contributed equally to this work

* Corresponding authors:

Carla Caddeo

Dept. of Scienze della Vita e dell'Ambiente, Sezione di Scienze del Farmaco, University of Cagliari, Via Ospedale 72, 09124 Cagliari, Italy

Tel.: +39 0706758582; fax: +39 0706758553; e-mail address: caddeoc@unica.it

Laura Pucci

52 Institute of Agricultural Biology and Biotechnology, CNR Pisa, Via Moruzzi 1, 56124 Pisa, Italy

53 Tel.: +39 0503153084; e-mail address: laura.pucci@ibba.cnr.it

54

ABSTRACT

Resveratrol and artemisinin, two naturally occurring compounds with a wide range of biological activities, have been reported to exert antitumor effects against several types of cancer. In this work, Eudragit-coated liposomes were developed to safely transport resveratrol and artemisinin through the gastrointestinal tract and target the intestine. The physico-chemical properties of the Eudragit-coated liposomes were assessed by light scattering and cryogenic transmission electron microscopy. Nanosized (around 100 nm), spherical or elongated, unilamellar vesicles were produced. The protective effect of the Eudragit coating was confirmed by assessing the physical stability of the vesicles in fluids mimicking the gastrointestinal environment. Furthermore, the vesicles were found to exert a pro-oxidant activity in intestinal adenocarcinoma cells, which resulted in a marked mortality due to the generation of reactive oxygen species (ROS). A time- and dose-dependent cell growth inhibitory effect was detected, with elevated ROS levels when resveratrol and artemisinin were combined. Therefore, the proposed formulations may represent a valuable means to counteract intestinal tumor growth.

Keywords: resveratrol; artemisinin; eudragit; liposomes; intestinal delivery; antitumor.

1. Introduction

The development of new drug therapies still remains time-consuming and costly. Hence, new strategies, approaches and technologies are needed to develop safe and successful therapies (Sun et al., 2016). Combinations of two or more compounds are an alternative approach to increase the success of a therapy, especially for cancer treatment (Li et al., 2014). The potentially favorable outcomes for synergism include: minimizing or slowing down the development of drug resistance, providing selective synergism against cancer target versus host, increasing the efficacy of the therapy, and reducing the dose of the drugs to avoid toxicity (Chou 2006). A large number of untapped and potentially therapeutic molecules with reduced side effects can be provided by traditional herbal medicines and the diet (Firestone and Sundar, 2009). Natural compounds, such as resveratrol and artemisinin, have gained great interest in the pharmaceutical research area due to their numerous health-promoting effects, coupled with safety profile and natural origin (Efferth, 2007; Caddeo et al., 2015). In particular, resveratrol was demonstrated to exert potent antitumor activity against several types of cancer by using numerous experimental models, including cell lines, animal models, and even clinical trials (Khan et al., 2013). Several studies have demonstrated that resveratrol can act as either an antioxidant or pro-oxidant, depending on the specific microenvironment, type of cells used and their basal redox state, treatment conditions, and concentration used (Alarcón de la Lastra and Villegas, 2007; Khan et al., 2013; Martins et al., 2014; Shaito et al., 2020). Such antioxidant/pro-oxidant activities seem to be responsible for the chemopreventive and anticancer properties of resveratrol (Alarcón de la Lastra and Villegas, 2007). Indeed, biphasic hormetic dose-dependent effects have been described: at low concentrations, resveratrol acts as an antioxidant that can protect from DNA damage and oxidative stress, and at high concentrations, it acts as a pro-oxidant promoting DNA damage while increasing oxidative stress. Low and high concentrations offer beneficial effects in the prevention of cancer formation

100 (chemopreventive) and in the treatment of cancer (cytotoxic), respectively (Calabrese et al. 2010;
101 Shaito et al., 2020).
102 Artemisinin, a sesquiterpene lactone from *Artemisia annua*, is widely used worldwide to combat
103 otherwise drug-resistant *Plasmodium* strains, cerebral malaria, and malaria in children, but it also
104 exhibits potent anticancer effects in a variety of human cancer cell model systems and in animal
105 models (Efferth, 2007; Firestone and Sundar, 2009; Ferreira et al., 2010). Artemisinin contains an
106 endoperoxide group that is essential for its activities. Artemisinin reacts with ferrous iron (Fe^{2+}) to
107 generate short-lived radical species (ROS), which have been linked to both the antiparasitic and
108 anticancer activities (Ferreira et al., 2010; Slezakova and Ruda-Kucerova, 2017). Although the
109 generation of ROS is one of the main mechanisms for the anticancer activity, there are many
110 cellular signaling pathways affected, which lead to growth inhibition by cell cycle arrest, apoptosis,
111 inhibition of angiogenesis, disruption of cell migration, and modulation of nuclear receptor
112 responsiveness (Firestone and Sundar, 2009).
113 The synergistic effect of resveratrol and artemisinin has been previously assessed in cancer cells
114 (HepG2 and HeLa cells) by Li et al. (2014). The combination of the two compounds was found to
115 markedly reduce cell viability and migration and to induce apoptosis, which was correlated with an
116 increase in intracellular ROS levels.
117 Differently from what has been proposed previously, in this work resveratrol and artemisinin were
118 combined to target tumors, more specifically intestinal tumors, by taking advantage of a delivery
119 system. Indeed, the two compounds were co-loaded in a phospholipid-based nanocarrier that is
120 expected to enhance their oral bioavailability (since they are poorly soluble in water) and stability in
121 physiological media, ensuring protection from gastrointestinal degradation and preventing
122 premature release. To this purpose, Eudragit-coated liposomes were used (Caddeo et al., 2019).
123 Eudragit® S100, a polyanionic copolymer of methacrylic acid and methyl metacrylate (1:1) that is
124 insoluble at gastric pH and dissolves above pH 7.0, was used to coat cationic liposomes loaded with

resveratrol and artemisinin, thus serving two purposes: protecting the vesicles from acidic degradation, and allowing the release of the payload in the region of the intestinal tract with near-neutral pH (i.e., the large intestine or colon).

The vesicular formulation was optimized and characterized to assess the main physico-chemical properties and the ability to resist the harsh conditions of the gastrointestinal tract. Additionally, the anti-proliferative activity of the formulation was investigated in human colonic adenocarcinoma HT-29 cells, with a focus on whether ROS overproduction might be a key factor in tumor cell growth inhibition.

2. Materials and methods

2.1. Materials

Phospholipon90G (>90% phosphatidylcholine; P90G) was purchased from Lipoid GmbH (Ludwigshafen, Germany). Eudragit® S100 (Eu) was a gift from Evonik Industries AG (Essen, Germany). Resveratrol (RSV), artemisinin (ART), stearylamine (SA), phosphate buffered saline (PBS), and all other reagents, if not otherwise specified, were purchased from Sigma-Aldrich/Merck (Milan, Italy).

2.2. Vesicle preparation and characterization

P90G, stearylamine, resveratrol and/or artemisinin (i.e., alone or in combination at the ratio of 1:1) were weighed in a glass vial and dispersed in PBS (Table 1). To obtain liposomes, the dispersions were sonicated (5 sec on and 2 sec off, 30 cycles; 13 microns of probe amplitude) with a Soniprep 150 (MSE Crowley, London, UK). To produce Eudragit-coated liposomes, 1 ml of the liposome dispersion was added dropwise to an equal volume of an Eudragit aqueous solution (0.1% w/v) under gentle stirring (Caddeo et al., 2019).

149 For comparative purposes, empty liposomes and empty Eudragit-coated liposomes (i.e., without
150 resveratrol and/or artemisinin) were also prepared.
151 All the samples were prepared and kept in the dark during the experimental time.
152 Vesicle formation and morphology were examined by cryogenic-transmission electron microscopy
153 (cryo-TEM). For the analysis, a thin aqueous film was formed by placing 5 µl of the vesicular
154 dispersion on a glow-discharged holey carbon grid, and then blotting the grid against filter paper.
155 The resulting thin sample film spanning the grid holes was vitrified by plunging the grid (kept at
156 100% humidity and room temperature) into ethane, maintained at its melting point with liquid
157 nitrogen, using a Vitrobot (FEI Company, Eindhoven, The Netherlands). The vitreous film was
158 transferred to a Tecnai F20 TEM (FEI Company) using a Gatan cryo-transfer (Gatan, Pleasanton,
159 CA), and the sample was observed in a low-dose mode. Images were acquired at 200 kV, at a
160 temperature of –170/–175 °C, using low-dose imaging conditions not exceeding 20 $e^{-}/Å^{2}$, with a
161 4096 × 4096 pixel CCD Eagle camera (FEI Company).
162 The average diameter, polydispersity index (P.I., a measure of the width of size distribution), and
163 zeta potential of the vesicles were determined by dynamic and electrophoretic light scattering using
164 a Zetasizer nano-ZS (Malvern Instruments, Worcestershire, UK). Samples ($n \geq 6$) were diluted with
165 PBS (1:100) and analyzed at 25 °C.
166 The vesicles were purified from the non-incorporated resveratrol/artemisinin by dialysis. Each
167 sample (2 ml) was loaded into Spectra/Por® tubing (12–14 kDa MW cut-off; Spectrum Laboratories
168 Inc., DG Breda, The Netherlands), previously rinsed in water, and dialyzed against PBS (1 l) for 2 h
169 to allow the removal of the non-incorporated compounds. The entrapment efficiency (EE),
170 expressed as the percentage of the amount of resveratrol/artemisinin initially used, was determined
171 by high performance liquid chromatography (Alliance 2690, Waters, Milan, Italy) after disruption
172 of unpurified and purified vesicles with methanol. Resveratrol and artemisinin contents were
173 assayed using a XSelect C18 column (3.5 µm, 4.6×150 mm, Waters), with a mobile phase made of

methanol and water (85:15, v/v) and a flow rate of 0.5 ml/min. A_{305} and A_{201} were measured for resveratrol and artemisinin quantitation, respectively.

2.3. Stability of the formulations

Since Eudragit-coated liposomes are intended for oral administration, their behavior in the gastrointestinal environment was evaluated *in vitro*. The mean size, P.I. and zeta potential were measured immediately after dilution (1:100 v:v) of the vesicles with an acidic medium simulating the gastric fluid (0.1 M HCl, pH 1.2) or a neutral medium simulating the intestinal fluid (pH 7.0), and after 2 or 6 h of incubation, respectively, at 37 ± 1 °C. 0.3 M NaCl was added to the media to regulate the ionic strength. Liposomes (i.e., without Eudragit coating) were tested as a reference.

Further, the stability of liposomes and Eudragit-coated liposomes was evaluated by long-term stability tests, i.e. by analyzing vesicle mean size, P.I. and zeta potential over three months at 25 ± 2 °C.

2.4. Human intestinal cell culture

Human colonic adenocarcinoma HT-29 cells (DSMZ, Germany) were cultured as previously described by Gabriele et al. (2018). Briefly, HT-29 were grown in Dulbecco's modified Eagle's medium/nutrient mixture F-12 (DMEM/F12) supplemented with 10% fetal bovine serum (FBS), 100 units/ml penicillin, and 100 µg/ml streptomycin, and maintained at 37 °C in a humidified 5% CO_2 incubator. All treatments were carried out using DMEM/F12 medium without phenol red and FBS, but containing antibiotics. The cells were serum-starved for 1 h prior to exposure to the formulations, previously diluted to reach the required concentrations of resveratrol/artemisinin (0.1, 1, 10, 20 µg/ml), for 6 or 24 h. For comparative purposes, ethanolic solutions of resveratrol and/or artemisinin were tested at the same concentrations as the liposomal formulations.

198 The MTT assay was performed to assess cell viability of cultured HT-29 upon different treatment
199 conditions, as previously described by Gabriele et al. (2016). In short, after 3 h of incubation with
200 MTT, the cells were lysed with a dimethylsulfoxide/isopropanol solution and the formazan crystals
201 were solubilized. The amount of formazan released from the cells was quantified by measuring the
202 optical density at 540 nm using a Victor^{TM} X3 Multilabel Plate Reader (Waltham, MA), and
203 correlated with the amount of metabolically active cells.
204
205 *2.5. Cellular ROS determination*
206 The cellular ROS were detected using 2,7-dichlorofluorescein diacetate (DCFH-DA) fluorescent
207 probe. After diffusion into viable cells, DCFH-DA is first deacetylated by cellular esterases to a
208 non-fluorescent compound (DCFH), then oxidized to DCF, a highly fluorescent compound, by ROS
209 activity (Gabriele et al., 2017). Briefly, HT-29 cells were seeded into a 96-well blackened
210 fluorescence plate and exposed to the formulations previously diluted to reach the required
211 concentrations of resveratrol/artemisinin (0.1, 1, 10, 20 μg/ml), for 6 and 24 h. For comparative
212 purposes, ethanolic solutions of resveratrol and/or artemisinin were tested at the same
213 concentrations as the liposomal formulations. Afterwards, the cells were rinsed with 1× PBS and
214 incubated with DCFH-DA (15 μM/well) for 30 min at 37 °C in the dark. DCFH-DA solution was
215 removed, HT-29 were rinsed with 1× PBS, and 2,2′-azobis(2-methylpropionamidine)
216 dihydrochloride (AAPH) was added to a final concentration of 1.2 mM/well. AAPH is a peroxyl
217 radical generator used as a positive control. ROS production was measured by fluorescence
218 intensity measurement by means of a Victor X3 Multilabel Plate Reader (λ_{ex} 485 nm, λ_{em} 535 nm).
219
220 *2.6. Statistical analysis of data*
221 Results are expressed as the mean ± standard deviation (SD). Statistical analysis of data was
222 performed using GraphPad Prism, version 6.00 for Windows (GraphPad Software, San Diego, CA)

by one-way analysis of variance (ANOVA). Unpaired Student's t-test was used for single comparisons. *P* values <0.05 were considered as statistically significant.

3. Results and discussion

3.1. Vesicle design and characterization

The present study was aimed at developing a vesicular formulation for the delivery of co-loaded resveratrol and artemisinin to the intestine. Eudragit-coated liposomes were used to increase the physical stability of the system, providing protection from gastric degradation and allowing pH-driven intestinal targeting, and to enhance the antitumor activity of resveratrol and artemisinin at cellular level. Furthermore, the potential synergistic effect of the two natural compounds was evaluated.

Resveratrol and artemisinin Eudragit-coated liposomes were prepared, characterized and compared with Eudragit-liposomes loaded with either resveratrol or artemisinin, liposomes loaded with resveratrol and/or artemisinin, empty Eudragit-liposomes and empty liposomes.

Light scattering results, summarized in Table 2, showed that empty liposomes were small in size (~80 nm), with adequate homogeneity (P.I. 0.24), and positive zeta potential (+18 mV), due to the charge carried by stearylamine. The loading of resveratrol and/or artemisinin did not alter these values ($p>0.05$), apart from the P.I. values, which were much lower (e.g., 0.17 for resveratrol+artemisinin liposomes; $p<0.05$). The coating of liposomes with Eudragit led to an increase in size and polydispersity (~140 nm and P.I.>0.3; $p<0.05$), and to a less positive zeta potential (+10 mV; $p < 0.05$), due to the negative charge of the polymer. The co-loading of resveratrol and artemisinin in Eudragit-coated liposomes mitigated the vesicle enlargement (~100 nm) induced by the polymer coating. An increase in vesicle size is closely related to the concentration of the polymer coating solution (Barea et al., 2010; Kim et al., 2018). In accordance

247 with previous works, a polymer concentration of 0.1% (w/v) was chosen to yield non-flocculating
248 polymer-coated liposomes (Klemetsrud et al., 2018; Caddeo et al., 2019).
249 The entrapment efficiency was high for both resveratrol and artemisinin (~87 and 91%,
250 respectively; Table 2), and the amount of the loaded compounds did not diminish during storage
251 over the course of three months ($p>0.05$).
252 Cryo-TEM observation of resveratrol+artemisinin Eudragit-coated liposomes confirmed the
253 formation of small, spherical or elongated, unilamellar vesicles (Figure 1). No significant
254 differences were observed in uncoated vesicles, loaded with either resveratrol or artemisinin, and
255 there was no evidence of free resveratrol/artemisinin crystals.
256
257 *3.2. Stability of the formulations*
258 The stability of vesicle dispersions, which is dependent on both formulation and manufacturing
259 method parameters, is critical to establish their safe and effective use. Therefore, the stability of the
260 prepared formulations was evaluated by monitoring the mean size, P.I. and zeta potential of the
261 vesicles over three months of storage, the results showing no significant variations ($p>0.05$).
262 In addition, the stability of the formulations was assessed under pH and ionic strength conditions
263 mimicking the gastrointestinal environment (Table 3). When uncoated liposomes were incubated at
264 pH 1.2 for 2 h, a moderate increase in size was observed (~100 vs. 80 nm), along with a slightly
265 lower polydispersity (P.I. ~0.21), regardless of the loaded compound. Under the same conditions,
266 Eudragit-coated liposomes remained unaltered: ~100 nm and P.I. 0.36 for resveratrol+artemisinin
267 Eudragit-coated liposomes and ~140 nm and P.I. 0.34 for resveratrol or artemisinin Eudragit-coated
268 liposomes. When the formulations were incubated at pH 7.0 for 6 h, neither liposomes nor Eudragit-
269 coated liposomes underwent any variations. Fluctuations of zeta potential values were detected as a
270 function of the presence of protons or salts in the gastric or intestinal medium. These findings

indicated that the Eudragit coating increased the physical stability of the vesicle formulations that, differently from uncoated liposomes, resisted the harsh conditions of the stomach.

3.3. Cytotoxicity and intracellular ROS production

The inhibitory effect of resveratrol/artemisinin formulations on colonic adenocarcinoma HT-29 cell growth was evaluated in terms of cell viability following 6- and 24-h exposure to increasing concentrations of resveratrol and artemisinin (0.1-20 μg/ml), alone or in combination.

After 6 h of treatment, resveratrol/artemisinin ethanolic solutions (used as references) did not affect HT-29 viability at any of the tested concentrations (Figure 2, panel A). Similarly, none of the liposome formulations caused cytotoxicity except for resveratrol+artemisinin Eudragit-coated liposomes at 1 μg/ml, which reduced cell viability by about 11% relative to the control cells (•••$p<0.001$).

On the other hand, significant cell mortality levels were detected following 24 h of exposure to 20 μg/ml of resveratrol and artemisinin ethanolic solution (~11-16%; ***$p<0.001$ and *$p<0.05$ vs. control, respectively), and a similar effect was also caused by resveratrol+artemisinin ethanolic solution at 1 μg/ml (~14%; **$p<0.01$ vs. control) (Figure 2, panel B). Moreover, resveratrol Eudragit-coated liposomes negatively impaired HT-29 growth at the highest concentration (~33% viability reduction relative to control; ***$p<0.001$), and artemisinin Eudragit-coated liposomes caused a notable decrease in HT-29 viability at concentrations ≥1 μg/ml (~25-53%; ***$p<0.001$ vs. control, for all the concentrations). As shown in Figure 2 (panel B), the incorporation of both resveratrol and artemisinin in Eudragit-coated liposomes caused about 16% and 37% reduction in HT-29 viability following 24 h of exposure to 10 and 20 μg/ml, respectively (***$p<0.001$ vs. control), leading to a higher cytotoxicity than resveratrol+artemisinin ethanolic solution. These findings demonstrated a higher efficacy of resveratrol+artemisinin incorporated in Eudragit-coated liposomes than resveratrol+artemisinin ethanolic solution. These results are probably linked to a

296 higher stability and controlled delivery of the two natural compounds, which led to a higher
297 cytotoxic effect resulting in higher mortality levels and growth inhibition of intestinal HT-29 cells.
298 As demonstrated by several studies, resveratrol can serve as either an antioxidant or pro-oxidant
299 agent, depending on the concentration and the specific microenvironment, and the pro-oxidant
300 activity seems to be responsible for the anticancer properties of resveratrol (Khan et al., 2013;
301 Alarcón de la Lastra and Villegas, 2007). Similarly, artemisinin showed anti-proliferative properties
302 on many cancer cell lines, such as colon, liver, prostate, and breast cancer, by operating through the
303 impairment of cytokines, oxidative stress increase, and inhibition of tumor invasion and migration
304 (Li at al., 2014). Moreover, as reported by Kim et al. (2015), artemisinin extracts from *Artemisia*
305 *annua* displayed good anti-inflammatory, antioxidant, and antimicrobial properties; therefore, as in
306 the case of resveratrol, the antitumor effect could be concentration-dependent.
307 In this study, we evaluated the effect of resveratrol/artemisinin formulations on the ROS production
308 in HT-29 cells by using a cell-permeable dye sensitive to the cellular redox state (DCFH-DA).
309 Intracellular ROS levels were determined following 6- and 24-h exposure to increasing
310 concentrations of resveratrol/artemisinin formulations (0.1-20 μg/ml), alone or in combination, and
311 the obtained results were normalized by viability values. As shown in Figure 3 A, following 6 h of
312 exposure to resveratrol and artemisinin solutions and Eudragit-coated liposomes, a decrease in ROS
313 levels was observed (•$p<0.05$ vs. control, i.e. AAPH-treated cells), except for 1 μg/ml resveratrol,
314 0.1 μg/ml resveratrol+artemisinin, 10 and 20 μg/ml resveratrol+artemisinin Eudragit-coated
315 liposomes, where no significant differences were found vs. control cells.
316 A significant ROS reduction was also observed, following 24 h of exposure, at the higher doses of
317 resveratrol and artemisinin in solution, alone or in combination (**$p<0.01$ vs. control) (Figure 3 B).
318 Conversely, while low doses of resveratrol and artemisinin Eudragit-coated liposomes reduced the
319 basal ROS level (antioxidant effect), the higher dose (20 μg/ml) caused a significant increase in the
320 cellular ROS production (pro-oxidant effect) (*$p<0.05$ vs. control). Besides, significantly higher

ROS levels were detected in HT-29 exposed to 20 μg/ml resveratrol+artemisinin Eudragit-coated liposomes in comparison with the control and the higher dose of resveratrol+artemisinin solution ($p<0.001$). Also, a trend of increasing ROS levels was observed following a 24-h exposure to 10 μg/ml resveratrol+artemisinin Eudragit-coated liposomes, but these results did not differ from the control cells (Figure 3 B).

As shown in Figure 3 B, the combination of resveratrol and artemisinin in Eudragit-coated liposomes at 10 and 20 μg/ml raised intracellular HT-29 ROS production more than resveratrol and artemisinin used alone. Notably, this increase was strongly evident following an exposure to 10 μg/ml resveratrol+artemisinin Eudragit-coated liposomes ($p<0.01$), but ROS levels were lower than in cells treated with 20 μg/ml dose ($p<0.01$). Our results are in agreement with those reported by Li et al. (2014), who demonstrated a synergistic anticancer effect of resveratrol and artemisinin combination via raised ROS production, cellular growth inhibition, and cell migration, as compared to the compounds used alone.

Taken together, our findings showed a superior pro-oxidant activity of resveratrol+artemisinin incorporated in Eudragit-coated liposomes than resveratrol+artemisinin in solution. Similar to what was supposed for HT-29 growth inhibition, presumably the incorporation of resveratrol and artemisinin in Eudragit-coated liposomes enhanced the stability and delivery of both compounds to the cells. Furthermore, we can hypothesize a synergistic effect of resveratrol and artemisinin. Indeed, resveratrol+artemisinin incorporated in Eudragit-coated liposomes at a concentration of 20 μg/ml exerted a significantly higher pro-oxidant effect than Eudragit-coated liposomes loaded with either resveratrol or artemisinin at a concentration of 10 μg/ml each ($p<0.0001$). This result is confirmed by the viability assay: Eudragit-coated liposomes loaded with resveratrol and artemisinin, at a total concentration of 20 μg/ml, induced a higher cytotoxicity than the Eudragit-coated liposomes loaded with resveratrol at 10 μg/ml ($p<0.0001$) or artemisinin at 10 μg/ml (not statistically significant).

4. Conclusions

The results of this work suggest that Eudragit-coated liposomes are an effective vesicle system for the incorporation, protection, and delivery of resveratrol and artemisinin. The vesicles showed stability under simulated gastrointestinal conditions, which confirms their feasible use for the oral delivery of the two natural compounds. Further, the *in vitro* results in human intestinal cancer cells displayed a time- and dose-dependent, synergistic growth inhibitory potential of the prepared formulations via an increase in ROS intracellular levels. These findings highlight the need for further research on the mechanisms of action of Eudragit-coated liposomes by assessing the release kinetics of resveratrol and artemisinin and the modulation of the expression of genes involved in cell death induced by the two natural compounds. These investigations will allow us to validate the antitumor potential of the proposed formulation and confirm its efficacy against intestinal cancer.

Acknowledgments

This research was partially supported by grants RTI2018-094579-B-I00 (Spanish Ministry of Science, Innovation and Universities Ministerio de Economía y Competitividad, Spain), which included FEDER funds, and 2017-SGR-9082014-SGR-938 (Generalitat de Catalunya, Spain).

References

Sun, W., Sanderson, P., Zheng, W., 2016. Drug combination therapy increases successful drug repositioning. Drug Discov. Today 21, 1189–1195.

Li, P., Yang, S., Dou, M., Chen, Y., Zhang, J., Zhao, X., 2014. Synergic effects of artemisinin and resveratrol in cancer cells. J. Cancer Res. Clin. Oncol. 140, 2065–2075.

Chou, T.C., 2006. Theoretical basis, experimental design, and computerized simulation of synergism and antagonism in drug combination studies. Pharmacol. Rev. 58, 621–681.

Firestone, G.L., Sundar, S.N., 2009. Anticancer activities of artemisinin and its bioactive derivatives. Expert Rev. Mol. Med. 11:e32.

Efferth, T., 2007. Willmar Schwabe Award 2006: antiplasmodial and antitumor activity of artemisinin - From bench to bedside. Planta Med. 73, 299–309.

Caddeo, C., Manconi, M., Cardia, M.C., Díez-Sales, O., Fadda, A.M., Sinico, C., 2015. Investigating the interactions of resveratrol with phospholipid vesicle bilayer and the skin: NMR studies and confocal imaging. Int. J. Pharm. 484, 138-145.

Khan, A., Chen, H., Wan, X., Tania, M., Xu, A., Chen, F., Zhang, D., 2013. Regulatory effects of resveratrol on antioxidant enzymes: a mechanism of growth inhibition and apoptosis induction in cancer cells. Mol. Cells 35, 219-225.

Alarcón de la Lastra, C., Villegas, I., 2007. Resveratrol as an antioxidant and pro-oxidant agent: mechanisms and clinical implications. Biochemical Society Transactions, Volume 35, part 5.

Martins, L.A., Coelho, B.P., Behr, G., Pettenuzzo, L.F., Souza, I.C., Moreira, J.C., Borojevic, R., Gottfried, C., Guma, F.C., 2014. Resveratrol induces pro-oxidant effects and time-dependent resistance to cytotoxicity in activated hepatic stellate cells. Cell Biochem. Biophys. 68, 247–257.

Shaito, A., Posadino, A.M., Younes, N., Hasan, H., Halabi, S., Alhababi, D., Al-Mohannadi, A., Abdel-Rahman, W.M., Eid, A.H., Nasrallah, G.K., Pintus, G., 2020. Potential adverse effects of resveratrol: a literature review. Int. J. Mol. Sci. 21, 2084.

389 Calabrese, E.J., Mattson, M.P., Calabrese, V., 2010. Resveratrol commonly displays hormesis:
390 occurrence and biomedical significance. Hum. Exp. Toxicol. 29, 980–1015.
391 Ferreira, J.F.S., Luthria, D.L., Sasaki, T., Heyerick, A., 2010. Flavonoids from *Artemisia annua* L.
392 as antioxidants and their potential synergism with artemisinin against malaria and cancer.
393 Molecules 15, 3135-3170.
394 Slezakova, S., Ruda-Kucerova, J., 2017. Anticancer activity of artemisinin and its derivatives.
395 Anticancer Research 37, 5995-6003.
396 Caddeo, C., Gabriele, M., Fernàndez-Busquets, X., Valenti, D., Fadda, A.M., Pucci, L., Manconi,
397 M., 2019. Antioxidant activity of quercetin in Eudragit-coated liposomes for intestinal delivery. Int.
398 J. Pharm. 565, 64–69.
399 Gabriele, M., Pucci, L., Julius, Á., Longo, V., 2018. Anti-inflammatory and antioxidant effects of
400 fermented whole wheat on TNFα-stimulated HT-29. J. Funct. Foods 45, 392-400.
401 Gabriele, M., Pucci, L., La Marca, M., Lucchesi, D., Della Croce, C.M., Longo, V., Lubrano, V.**,**
402 2016. A fermented bean flour extract downregulates LOX-1, CHOP and ICAM-1 in HMEC-1
403 stimulated by ox-LDL. Cell. Mol. Biol. Lett. 21:10.
404 Gabriele, M., Frassinetti, S., Caltavuturo, L., Montero, L., Dinelli, G., Longo, V., Di Gioia, D.,
405 Pucci, L., 2017. Citrus bergamia powder: Antioxidant, antimicrobial and anti-inflammatory
406 properties. J. Funct. Foods 31, 255-265.
407 Barea, M.J., Jenkins, M.J., Gaber, M.H., Bridson, R.H., 2010. Evaluation of liposomes coated with
408 a pH responsive polymer. Int. J. Pharm. 402, 89–94.
409 Kim, J.H., Shin, D.H., Kim, J.-S., 2018. Preparation, characterization, and pharmacokinetics of
410 liposomal docetaxel for oral administration. Arch. Pharm. Res. 41, 765–775.
411 Klemetsrud, T., Kjøniksen, A.-L., Hiorth, M., Jacobsen, J., Smistad, G., 2018. Polymer coated
412 liposomes for use in the oral cavity – a study of the in vitro toxicity, effect on cell permeability and
413 interaction with mucin. J. Liposome Res. 28(1), 62–73.

414 Kim, W.-S., Choi, W.J., Lee, S., Kim, W.J., Lee, D.C., Sohn, U.D., Shin, H.-S., Kim, W., 2015.
415 Anti-inflammatory, Antioxidant and Antimicrobial Effects of Artemisinin Extracts from *Artemisia*
416 *annua* L. Korean J. Physiol. Pharmacol. 19, 21-27.
417

Figure captions

Figure 1. Cryo-TEM images of resveratrol and artemisinin Eudragit-coated liposomes.

Figure 2. Effect of 6- and 24-h exposure to increasing doses of resveratrol/artemisinin ethanolic solutions vs. the liposomal formulations on HT-29 cell viability evaluated by MTT assay.

The concentration of resveratrol+artemisinin samples corresponds to the sum of equal concentrations of the two compounds.

• symbol indicates values statistically different from 6-h untreated cells (Control): •$p<0.05$, ••$p<0.01$, •••$p<0.001$; *symbol indicates values statistically different from 24-h untreated cells (control): $^{*}p<0.05$, $^{**}p<0.01$, $^{***}p<0.001$.

Figure 3. Effect of 6- and 24-h exposure to increasing doses of resveratrol/artemisinin ethanolic solutions vs. the liposomal formulations on ROS production in HT-29 cells.

The concentration of resveratrol+artemisinin samples corresponds to the sum of equal concentrations of the two compounds.

• symbol indicates values statistically different from 6-h untreated cells exposed to AAPH (Control): •$p<0.05$, ••$p<0.01$, •••$p<0.001$; * symbol indicates values statistically different from 24-h untreated cells exposed to AAPH (Control): $^{*}p<0.05$, $^{**}p<0.01$, $^{***}p<0.001$.

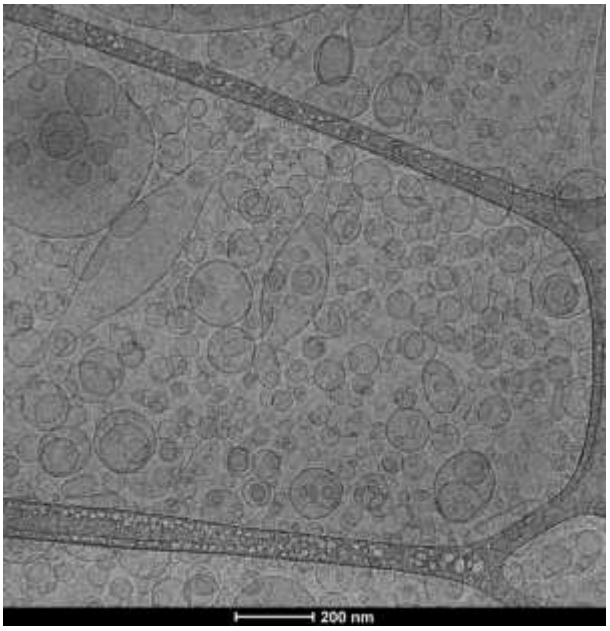
200 nm

436

437

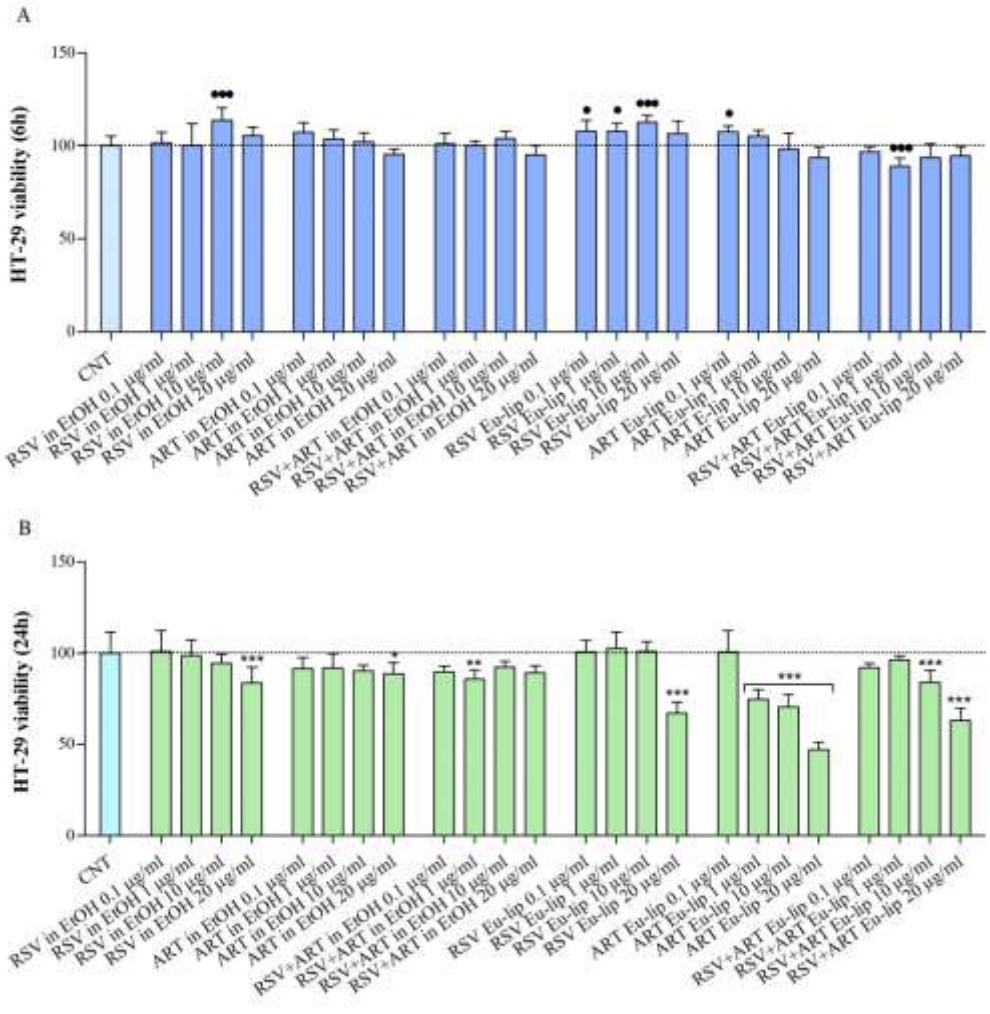
A
HT-29 viability (6h)
150
100
50
0
CNT
RSV in EtOH 0.1 µg/ml
RSV in EtOH 1 µg/ml
RSV in EtOH 10 µg/ml
RSV in EtOH 20 µg/ml
ART in EtOH 0.1 µg/ml
ART in EtOH 1 µg/ml
ART in EtOH 10 µg/ml
ART in EtOH 20 µg/ml
RSV+ART in EtOH 0.1 µg/ml
RSV+ART in EtOH 1 µg/ml
RSV+ART in EtOH 10 µg/ml
RSV+ART in EtOH 20 µg/ml
RSV Eu-lip 0.1 µg/ml
RSV Eu-lip 1 µg/ml
RSV Eu-lip 10 µg/ml
RSV Eu-lip 20 µg/ml
ART Eu-lip 0.1 µg/ml
ART Eu-lip 1 µg/ml
ART Eu-lip 10 µg/ml
ART Eu-lip 20 µg/ml
RSV+ART Eu-lip 0.1 µg/ml
RSV+ART Eu-lip 1 µg/ml
RSV+ART Eu-lip 10 µg/ml
RSV+ART Eu-lip 20 µg/ml
B
HT-29 viability (24h)
150
100
50
0
CNT
RSV in EtOH 0.1 µg/ml
RSV in EtOH 1 µg/ml
RSV in EtOH 10 µg/ml
RSV in EtOH 20 µg/ml
ART in EtOH 0.1 µg/ml
ART in EtOH 1 µg/ml
ART in EtOH 10 µg/ml
ART in EtOH 20 µg/ml
RSV+ART in EtOH 0.1 µg/ml
RSV+ART in EtOH 1 µg/ml
RSV+ART in EtOH 10 µg/ml
RSV+ART in EtOH 20 µg/ml
RSV Eu-lip 0.1 µg/ml
RSV Eu-lip 1 µg/ml
RSV Eu-lip 10 µg/ml
RSV Eu-lip 20 µg/ml
ART Eu-lip 0.1 µg/ml
ART Eu-lip 1 µg/ml
ART Eu-lip 10 µg/ml
ART Eu-lip 20 µg/ml
RSV+ART Eu-lip 0.1 µg/ml
RSV+ART Eu-lip 1 µg/ml
RSV+ART Eu-lip 10 µg/ml
RSV+ART Eu-lip 20 µg/ml

438

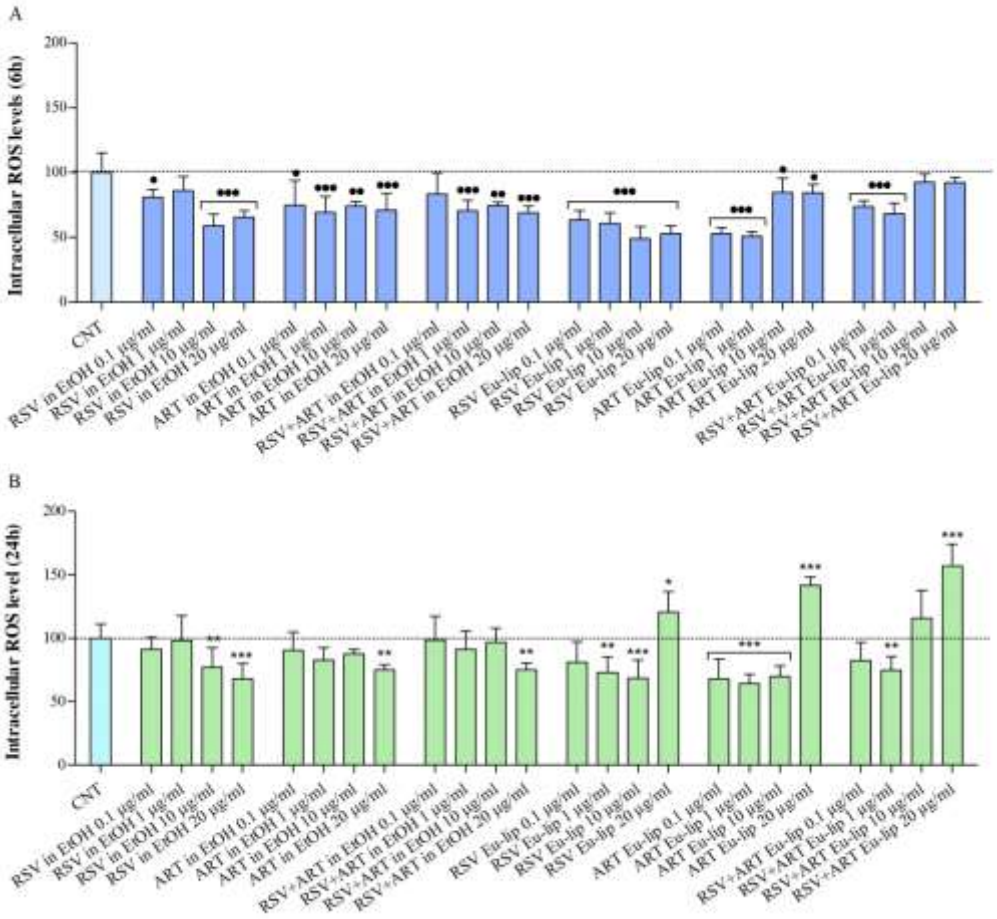
A
Intracellular ROS levels (6h)
200
150
100
50
0
CNT
RSV in EtOH 0.1 μg/ml
RSV in EtOH 1 μg/ml
RSV in EtOH 10 μg/ml
RSV in EtOH 20 μg/ml
ART in EtOH 0.1 μg/ml
ART in EtOH 1 μg/ml
ART in EtOH 10 μg/ml
ART in EtOH 20 μg/ml
RSV+ART in EtOH 0.1 μg/ml
RSV+ART in EtOH 1 μg/ml
RSV+ART in EtOH 10 μg/ml
RSV+ART in EtOH 20 μg/ml
RSV Eu-lip 0.1 μg/ml
RSV Eu-lip 1 μg/ml
RSV Eu-lip 10 μg/ml
RSV Eu-lip 20 μg/ml
ART Eu-lip 0.1 μg/ml
ART Eu-lip 1 μg/ml
ART Eu-lip 10 μg/ml
ART Eu-lip 20 μg/ml
RSV+ART Eu-lip 0.1 μg/ml
RSV+ART Eu-lip 1 μg/ml
RSV+ART Eu-lip 10 μg/ml
RSV+ART Eu-lip 20 μg/ml
B
Intracellular ROS level (24h)
200
150
100
50
0
CNT
RSV in EtOH 0.1 μg/ml
RSV in EtOH 1 μg/ml
RSV in EtOH 10 μg/ml
RSV in EtOH 20 μg/ml
ART in EtOH 0.1 μg/ml
ART in EtOH 1 μg/ml
ART in EtOH 10 μg/ml
ART in EtOH 20 μg/ml
RSV+ART in EtOH 0.1 μg/ml
RSV+ART in EtOH 1 μg/ml
RSV+ART in EtOH 10 μg/ml
RSV+ART in EtOH 20 μg/ml
RSV Eu-lip 0.1 μg/ml
RSV Eu-lip 1 μg/ml
RSV Eu-lip 10 μg/ml
RSV Eu-lip 20 μg/ml
ART Eu-lip 0.1 μg/ml
ART Eu-lip 1 μg/ml
ART Eu-lip 10 μg/ml
ART Eu-lip 20 μg/ml
RSV+ART Eu-lip 0.1 μg/ml
RSV+ART Eu-lip 1 μg/ml
RSV+ART Eu-lip 10 μg/ml
RSV+ART Eu-lip 20 μg/ml

Table 1. Composition of the liposomal formulations.

Formulation	P90G	SA	RSV	ART	PBS	Eu in H_2O
Empty liposomes	120 mg	6 mg			1 ml	
RSV liposomes	120 mg	6 mg	5 mg		1ml	
ART liposomes	120 mg	6 mg		5 mg	1 ml	
RSV+ART liposomes	120 mg	6 mg	2.5 mg	2.5 mg	1 ml	
Empty Eu-coated liposomes	120 mg	6 mg			1 ml	0.1% p/v
RSV Eu-coated liposomes	120 mg	6 mg	5 mg		1 ml	0.1% p/v
ART Eu-coated liposomes	120 mg	6 mg		5 mg	1 ml	0.1% p/v
RSV+ART Eu-coated liposomes	120 mg	6 mg	2.5 mg	2.5 mg	1 ml	0.1% p/v

P90G, phospholipid
SA, stearylamine
RSV, resveratrol
ART, artemisinin
PBS, phosphate buffered saline
Eu, Eudragit® S100

Table 2. Characteristics of empty, resveratrol-, artemisinin-, resveratrol+artemisinin liposomes and Eudragit-coated liposomes: mean diameter (MD), polydispersity index (P.I.), zeta potential (ZP), and entrapment efficiency (E). Each value represents the mean ± SD ($n \geq 6$). * values statistically different ($p<0.05$) from uncoated liposomes; # value statistically different ($p<0.05$) from empty liposomes.

Formulation	MD nm ± SD	P.I.	ZP mV ± SD	E % ± SD
Empty liposomes	77 ± 5.9	0.24 ± 0.09	+18 ± 1.6	--
RSV liposomes	82 ± 8.2	0.19 ± 0.02	+17 ± 1.6	84 ± 1.1
ART liposomes	81 ± 4.9	0.19 ± 0.02	+16 ± 1.4	90 ± 5.3
RSV+ART liposomes	82 ± 4.7	#0.17 ± 0.02	+17 ± 1.0	RSV 87 ± 1.9 ART 89 ± 6.3
Empty Eu-coated liposomes	*143 ± 24.8	*0.33 ± 0.03	*+10 ± 1.3	--
RSV Eu-coated liposomes	*148 ± 13.9	*0.37 ± 0.05	*+10 ± 0.9	86 ± 1.7
ART Eu-coated liposomes	*138 ± 9.9	*0.32 ± 0.06	*+10 ± 1.1	94 ± 4.7
RSV+ART Eu-coated liposomes	*103 ± 8.3	*0.36 ± 0.05	*+10 ± 0.7	RSV 90 ± 2.2 ART 91 ± 8.5

Table 3. Mean diameter, polydispersity index (P.I.) and zeta potential (ZP) of resveratrol-, artemisinin-, resveratrol+artemisinin liposomes and Eudragit-coated liposomes diluted and incubated with gastro-intestinal media at 37 °C. The measurements were carried out immediately after dilution (t_0) and after 2 (t_{2h}) or 6 h (t_{6h}) of incubation at pH 1.2 or 7.0 with high ionic strength (0.3 M NaCl). Mean values ± SDs are reported ($n \geq 6$).

Formulation	pH	Time	MD (nm)	P.I.	ZP (mV)
RSV liposomes	**1.2**	t_0	98 ± 4.1	0.22 ± 0.02	+13 ± 0.9
		t_{2h}	104 ± 6.0	0.22 ± 0.03	+14 ± 1.6
	7.0	t_0	84 ± 2.0	0.19 ± 0.02	+7 ± 1.0
		t_{6h}	83 ± 3.2	0.19 ± 0.02	+7 ± 0.8
ART liposomes	**1.2**	t_0	100 ± 5.3	0.21 ± 0.02	+13 ± 1.1
		t_{2h}	105 ± 2.7	0.22 ± 0.04	+13 ± 0.6
	7.0	t_0	80 ± 0.9	0.19 ± 0.03	+7 ± 0.9
		t_{6h}	84 ± 2.8	0.20 ± 0.02	+6 ± 1.3
RSV+ART liposomes	**1.2**	t_0	103 ± 2.1	0.22 ± 0.02	+14 ± 0.7
		t_{2h}	103 ± 4.2	0.21 ± 0.04	+13 ± 2.1
	7.0	t_0	82 ± 3.6	0.17 ± 0.02	+8 ± 1.7
		t_{6h}	81 ± 2.6	0.18 ± 0.02	+7 ± 1.1
RSV Eu-coated liposomes	**1.2**	t_0	145 ± 4.8	0.36 ± 0.03	+13 ± 1.5
		t_{2h}	143 ± 5.8	0.36 ± 0.04	+13 ± 0.7
	7.0	t_0	140 ± 4.1	0.37 ± 0.02	+7 ± 1.2
		t_{6h}	146 ± 2.6	0.38 ± 0.02	+8 ± 1.3
ART Eu-coated liposomes	**1.2**	t_0	135 ± 3.8	0.32 ± 0.02	+13 ± 0.2
		t_{2h}	140 ± 4.5	0.31 ± 0.05	+13 ± 0.5
	7.0	t_0	140 ± 4.2	0.33 ± 0.03	+7 ± 0.7
		t_{6h}	137 ± 3.9	0.32 ± 0.03	+7 ± 1.1
RSV+ART Eu-coated liposomes	**1.2**	t_0	105 ± 2.0	0.37 ± 0.03	+13 ± 0.6
		t_{2h}	106 ± 1.8	0.35 ± 0.02	+14 ± 0.7
	7.0	t_0	103 ± 2.7	0.36 ± 0.02	+7 ± 1.0
		t_{6h}	100 ± 4.0	0.35 ±0.02	+8 ± 0.4